Phase Shift Keying Using Optical Delay Modulation for Millimeter-Wave Fiber-Optic Radio Links

Yoshiyuki Doi, Seiji Fukushima, *Member, OSA*, Tetsuichiro Ohno, *Member, IEEE*, Yutaka Matsuoka, *Member, IEEE*, and Hiroaki Takeuchi

***Abstract*—We propose a novel phase shift keying technique that uses optical delay modulation for fiber-optic radio links. Using only a 2 × 1 switch and a delay line, this technique enables modulation of a millimeter-wave carrier at bit rates of several gigabits per second or higher, where high-speed devices are not needed. Binary phase shift keying (2PSK) was experimentally demonstrated. 2-Gb/s data signal on a 40-GHz carrier was transmitted over a 5-km optical fiber without any error. The coherent crosstalk noise, due to insufficient extinction ratio of optical switches, was evaluated. The 2PSK modulation technique can be extended to multiphase shift-keying modulation.**

***Index Terms*—Coherent crosstalk noise, millimeter-wave, modulation, multiple phase shift keying (MPSK), optical delay lines, optic radio links, phase shift keying (PSK), subcarrier multiplexing (SCM).**

I. Introduction

WIRELESS access systems and wireless local area networks using millimeter-wave (mm-wave) bands are attractive because of their potential for high-bit rate communications. Since mm-wave radio signal is drastically lost in the air, the diameter of each cell zone will be as small as 100 m. Therefore, many access stations are needed to cover wide areas and each must be equipped with an antenna, amplifier, and other costly electronic devices. Using fiber-optic radio links would make the acces sstations simpler and cheaper [1], [2]. Once mm-wave signal is multiplexed with light, it is transported over a long distance through an optical fiber. With such a system, the number of electronic devices at access stations could be decreased because such devices could be installed in the central station. As a result, the entire system cost could be reduced.

Many fiber-optic radio link systems have been demonstrated [3], [4]; however, they have not fully utilized the advantages of mm-wave systems, such as their, high-bit-rate operation. In [3], data signal on a mm-wave carrier is generated before it is introduced a high-speed optical modulator. In [4], data signal and carrier signal are transported in a fiber separately and are mixed after photodetection. Both approaches employ mm-wave mixer for phase modulation. Under current technology, the mm-wave mixer is extremely expensive; hence, the system cost using such modulators is very high.

This paper reports a novel modulation technique based on a proposal in [5]. It can modulate microwave or mm-wave signals at a bit rate of a few gigabits per second without the need for high-speed electronic devices. Our modulator can be constructed with a 2 × 1 optical switch and an optical delay line. Binary phase shift-keying (2PSK) modulation is demonstrated, with which 2-Gb/s data on a 40-GHz carrier is transmitted over a 5-km optical fiber without any error. We measured coherent crosstalk noise due to the insufficient extinction ratio of optical switches. A configuration of the modulator for multiple phase shift keying (MPSK) is proposed as an extension of the 2PSK modulator.

Manuscript received June 9, 1999; revised November 12, 1999.

The authors are with NTT Photonics Laboratories, Kanagawa-ken, 243-0198, Japan.

Publisher Item Identifier S 0733-8724(00)02197-6.

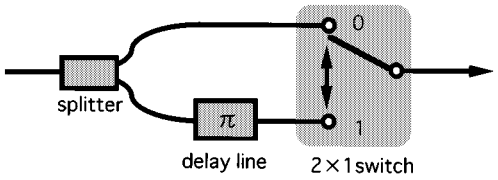

Fig. 1. The configuration of the 2PSK modulator.

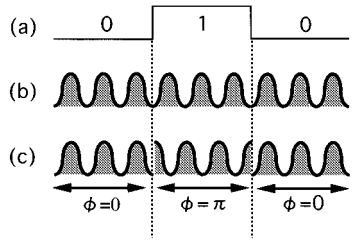

Fig. 2. Phase shift of the input and output intensity of the SCM light. (a) The logic value of input data, (b) the input light intensity, and (c) the output light intensity. Output SCM light has a phase of 0 or π according to input data.

II. Principle of 2PSK Modulation

Fig. 1 shows the configuration of 2PSK modulator. It consists of a splitter, an optical delay line, and a 2 × 1 switch. The first feature of this modulator is that mm-wave subcarrier multiplexing (SCM) light is phase-modulated optically. The delay corresponds to the π phase of a mm-wave carrier.

SCM light is input and then divided into two paths. The phase of π is added only at the lower path. The light beams are incident into the 2 × 1 switch and the switch selects one of the two beams. The upper path is chosen for an input data of false or 0, for example. The output light intensity is expressed as

$$\begin{cases} P_0 \cos \omega_n t, & \text{for data 0} \\ P_0 \cos(\omega_n t - \pi), & \text{for data 1} \end{cases} \tag{1}$$

where ω_n is angular frequency of the subcarrier and P_0 is light intensity amplitude. Fig. 2 shows the phase shift of the input and output intensities of the SCM light: 1) is the logic value of

input data, 2) the input light intensity, and 3) the output light intensity. The output SCM light has a phase of 0 or π according to the input data.

The second feature is that none of the devices in this configuration have to operate at a high carrier frequency in the mm-wave band. We can use optical devices based on either the electrooptic effect or electroabsorption effect 2×1 switch as long as they can switch at the data rate of baseband signal. Our technique provides very high bit rate data, so a time-division multiplexing (TDM) technique can be also employed for multiple access. Furthermore, there is no practical limitation on the carrier frequency in the micro- and mm-wave bands because only an adjustment of the delay length enables wide-carrier-frequency range application.

The third feature of this configuration is that we can apply many kinds of SCM light sources. A mode-locked semiconductor laser is one candidate [6], and light pulses with a terahertz repetition have been observed [7]. Other candidates are external modulators [8]–[10] used in combination with continuous-wave (CW) laser diodes (LD's). Single sideband techniques [11]–[14] are also applicable to overcome chromatic dispersion in fibers.

Our configuration is suitable for monolithic integration because the 2×1 switch and the delay line can be manufactured on a lithium niobate ($LiNbO_3$) substrate. The delay line length is shorter than a few mm at the mm-wave band, which will fit on the $LiNbO_3$ substrate with an optical switch. Such an integrated modulator can reduce the loss, cost, and system complexity.

This 2PSK configuration can be extended to MPSK, which will be described in detail in Section V.

III. 2PSK Experiments

A. Setup

The setup for the 2PSK modulation experiment is shown in Fig. 3. The parts enclosed by the dotted lines are referred to as the central station (CS), access station (AS), and remote terminal (RT).

SCM light is generated and modulated by the data signal at the CS. An integrated light source (ILS) was employed as a subcarrier generator. The ILS is a laser diode (LD) monolithically integrated with an electroabsorption (EA) modulator [15]. The maximum modulation frequency was 40 GHz at a wavelength of 1.55 μm. To obtain a high extinction ratio, bias voltage was set at -2.6 V, and a carrier of 40-GHz frequency with 2-V peak-to-peak voltage was applied to the EA modulator. The LD was operated at a current of 30 mA and its average light output power was -5 dBm. The shaded block in the CS in Fig. 3 is the 2PSK modulator. It consists of an optical splitter, two $LiNbO_3$ Mach–Zehnder modulators (MZM-1 and MZM-2), a delay line, a polarization controller (POL), and a combiner. A pulse pattern generator (PPG) feeds pulses into the two MZM's.

SCM light divided into two paths, one with and the other without a delay line, is incident into the two MZM's. The delay line was placed after an MZM (here, MZM-2) because the light polarization could be disturbed if it were set before the MZM. The set of the two MZM's and combiner are regarded as a 2×1 switch when the MZM's are operated complementarily. The voltage-transmittance curve of the MZM is shown in Fig. 4. It

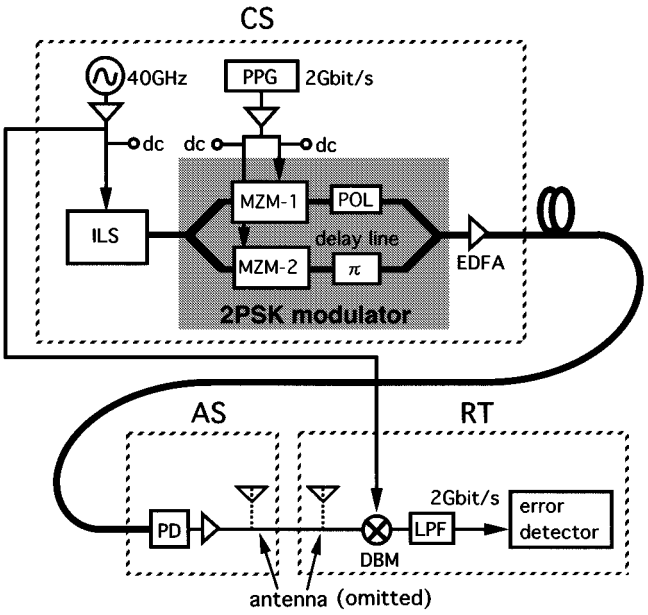

Fig. 3. The setup for the 2PSK modulation experiment. The carrier frequency and bit rate are 40 GHz and 2 Gb/s, respectively. The shaded block is the 2PSK modulator. ILS: integrated light source, MZM: Mach–Zender modulator, PPG: pulse pattern generator, POL: polarization controller, EDFA: Erbium doped fiber amplifier, PD: photodiode, LPF: low-pass filter.

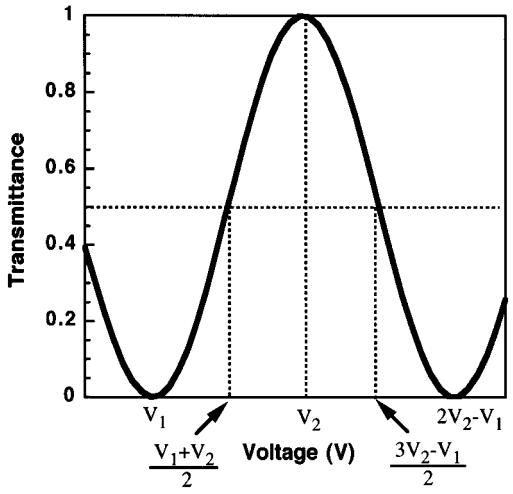

Fig. 4. The transmittance of the MZM. Bias voltage of MZM's is set at $3(V_2 - V_1)/2$ for MZM-1 and $(V_1 + V_2)/2$ for MZM-2.

varies periodically against the voltage and in the form of a sinusoidal function. V_1 and $2V_2 - V_1$ are voltages for minimum transmittance, and V_2 is the voltage for maximum transmittance. We assume that the bias voltages are set at $(3V_2 - V_1)/2$ for MZM-1 and $(V_1 + V_2)/2$ for MZM-2. The transmittance becomes 0.5 in both MZM's. Data signal input to each MZM simultaneously has voltage of $(V_2 - V_1)/2$ for a logic value of 1 and $-(V_2 - V_1/2)$ for a logic value of 0. The peak-to-peak voltages of the signal, $V_2 - V_1$, correspond to the half-wavelength voltage $(V\pi)$ of the MZM's, which was approximately 3 V in the experiments. The two MZM's operate as a 2×1 switch, whose operation is summarized in Table I. The voltage of MZM-1, V_{MZM1}, is V_2 and that of MZM-2, V_{MZM2}, is V_1 for the logic value of 0, and V_{MZM1} is $2V_2 - V_1$ and V_{MZM2} is V_2 for the logic value of 1. Taking a logic value of 0 as an example,

the transmittance status of MZM-1, T_{MZM1}, is on and the phase delay provided in this configuration becomes 0. In contrast for a logic value of 1, T_{MZM1} is off and delay is π.

A variable delay line was used for precisely adjusting phase. Its length was 3.75 mm in th air for a 40-GHz carrier. A POL was inserted to prevent coherent crosstalk noise, which causes power variation of a detected mm-wave carrier. The POL is adjusted for the polarizations of two lights to be orthogonal. The light pulses are amplified by an erbium-doped fiber amplifier (EDFA) and transmitted to the AS. A p-i-n-PD (NEL KEPD2525) was used for photo detection. In this experiment, antennas between the AS and RT were omitted because our main purpose is to confirm 2PSK modulation in the CS. After the detected signal was amplified, it was sent to the RT. The RT consists of a double-balanced mixer (DBM) and a low-path filter (LPF), which together function as a synchronous detection receiver. To measure the detected signal, we used a spectrum analyzer, a sampling oscilloscope, and an error detector.

B. Results

The carrier frequency and bit rate were 40 GHz and 2 Gb/s, respectively. Fig. 5 shows the results of back-to-back experiments. Input light power to the PD was -4.2 dBm. Fig. 5(a) shows the output waveform signal from the AS. The input data to the 2PSK modulator is the repetition pulse of the logic values of 1 and 0. A π-phase change is observed near the center and indicates successful 2PSK modulation. Fig. 5(b) shows the spectrum of the modulated carrier when 2-Gb/s pseudorandom bit stream (PRBS) signal is applied as the data. A 4-GHz main lobe width shows that the carrier is modulated by the data signal whose bit rate is 2 Gbit/s. The peak power of the main lobe is -17 dBm. Fig. 5(c) shows an eye diagram of a demodulated PRBS signal. The eye is clearly open with a peak-to-peak voltage of 200 mV.

The dependence of bit error rate on the optical power is shown in Fig. 6. Error-free mm-wave transmission is also confirmed using a 5-km dispersion shifted fiber (DSF). Interpolation of the line indicates that minimum input light power at the error rate of 1×10^{-9} were -13.9 dBm for the DSF and -13.7 dBm for the back-to-back fiber. There are almost no differences in the detected carrier power of the back-to-back fiber and DSF. No error rate floor is seen in the measured range. This means that the error rate will be decreased as the gain of an electronic amplifier is increased. According to a calculation of dispersion effect [16]–[18], the transmission length is limited mainly by the chromatic dispersion when the ILS is used, although the length of 5 km is sufficient for some applications such as a wireless local area network. For longer applications, some configurations [11]–[14] can be employed instead of the ILS in order to overcome fiber dispersion problems even if a single-mode fiber (SMF) is used.

The insertion loss of the 2PSK modulator was 15 dB, which includes 3-dB splitting loss of the input light, 8-dB MZM loss, and 3-dB coupling loss of the optical coupler. Since these losses arise from insufficient coupling at connections, the practical loss can be reduced by monolithically integrating all devices.

TABLE I
2×1 SWITCH OPERATION. V_{MZM1}: THE VOLTAGE OF MZM-1, V_{MZM2}: THE VOLTAGE OF MZM-2, T_{MZM1}: THE TRANSMITTANCE STATUS OF MZM-1, T_{MZM2}: THE TRANSMITTANCE STATUS OF MZM-2, ϕ THE PHASE OF SUBCARRIER SIGNAL

Data	V_{MZM1}	V_{MZM2}	T_{MZM1}	T_{MZM2}	ϕ
0	V_2	V_1	on	off	0
1	$2V_2$-V_1	V_2	off	on	π

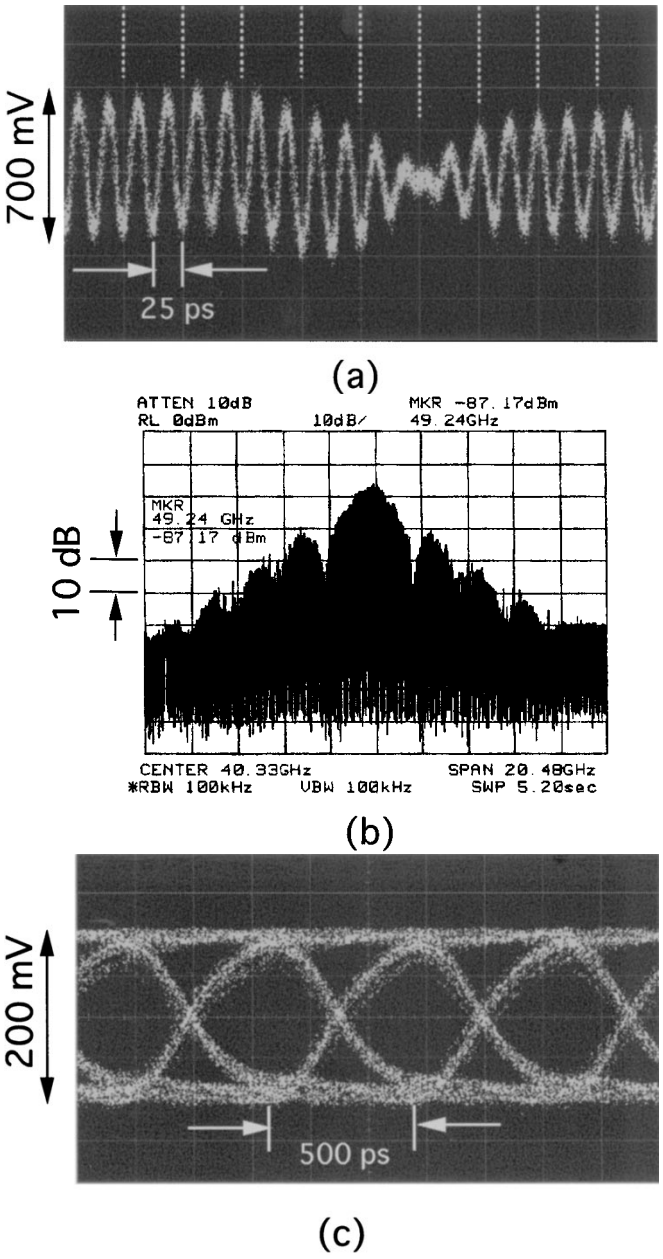

Fig. 5. The results of back-to-back, in which input light power was -4.2 dBm. (a) The output waveform signal from AS, where an input data to the 2PSK modulator is the repetition pulse of the logic value of 1 and 0. (b) The spectrum when pseudo-random bit stream signal is used. The division is 2 GHz for the frequency axis and 10 dB for the power axis. At the frequency of 40 GHz, the peak power of the main lobe is -17 dBm. (c) Eye-diagram of a demodulated pseudo-random bit stream signal. The eye is open with peak-to-peak voltage of 200 mV.

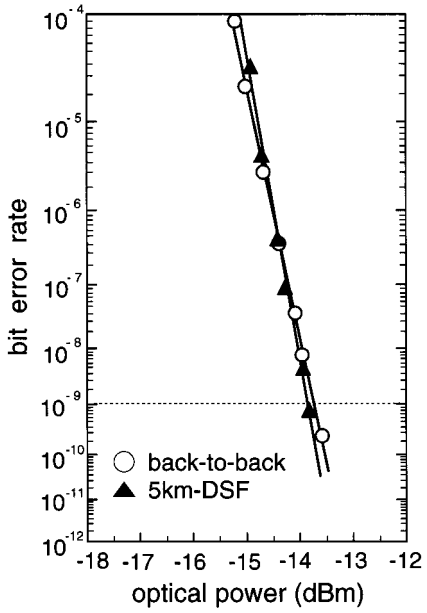

Fig. 6. BER dependence on the optical power.

IV. Discussion: Coherent Crosstalk Noise

Becuse of the insufficient extinction ratio of the MZM's, light coupling at the combiner causes coherent cross talk noise, and therefore, the detected signal becomes noisy. Here, we analyze the noise or power instability theoretically and compare it with the experimental results.

The two optical fields of two paths just before the 2 × 1 switch, E_1 and E_2, are defined by

$$E_1 = A\sqrt{1+m\cos\omega_n t}e^{j(\omega_0 t+\phi_1)} \tag{2}$$

$$E_2 = A_2\sqrt{1+m\cos\omega_n t}e^{j(\omega_0 t+\phi_2)} \tag{3}$$

where A_1 and A_2 are the field amplitudes of the light, ω_0 is the angular frequency of the light, ω_n is the angular frequency of the mm-wave subcarrier, m is the modulation index, and ϕ_1 and ϕ_2 are the phase of the light of fields E_1 and E_2, respectively. The relationship between A_1 and A_2 is expressed as

$$A_2^2 = \beta A_1^2 \tag{4}$$

where β is the extinction ratio of the 2 × 1 switch. If the lights of the two paths are polarized in parallel, the combined optical field E is given by

$$\begin{aligned} E &= E_1 + E_2 \\ &= \sqrt{1+m\cos\omega_n t}\{A_1 e^{j(\omega_0 t+\phi_1)} + A_2 e^{j(\omega_0 t+\phi_2)}\}. \end{aligned} \tag{5}$$

The detected current I is represented as

$$\begin{aligned} I \propto E\cdot E^* = A_1^2(1+m\cos\omega_n t) \\ \cdot\{1+\beta+2\sqrt{\beta}\cos(\phi_1-\phi_2)\}. \end{aligned} \tag{6}$$

The last term in (6), $2\sqrt{\beta}\cos(\phi_1-\phi_2)$, indicates the noise or power instability in the modulator. If the phase difference, $\phi_1-\phi_2$, changes slowly, the power instability of a mm-wave carrier is obsrved. In contrast, the variation is regarded as noise when the phase difference changes rapidly. We define the power variation γ as

$$\gamma = \left(\frac{I_{\max}+I_{\min}}{I_{\max}-I_{\min}}\right)^2 \tag{7}$$

where $I_{\max}$ and $I_{\min}$ are the maximum and minimum of current intensities, respectively. In (6), the current becomes $I_{\max}$ when $\cos(\phi_1-\phi_2)=1$ and $I_{\min}$ when $\cos(\phi_1-\phi_2)=-1$. From (6) and (7)

$$\gamma = \frac{(1+\beta)^2}{4\beta}. \tag{8}$$

The typical extinction ratio of the 2 × 1 switch is over 20 dB, and thus it is regarded that $\beta \gg 1$. Under this assumption, (8) can be written $\gamma = (\beta/4)$, which shows that γ is proportional to β.

Fig. 7 shows the experimental setup to verify the calculated variation γ. Instead of using a 2 × 1 switch, we inserted an optical attenuator into a path and the extinction ratio β was adjusted by the attenuation value. The two light polarizations were parallel for the worst-case consideration. The dependence of the carrier current of the detected signal, $I_{\max}$ and $I_{\min}$, on the extinction ratio is shown in Fig. 8. The variation of carrier signal is suppressed as the extinction ratio becomes higher. The experimental γ value was obtained by substituting $I_{\max}$ and $I_{\min}$ into (7). Fig. 9 shows the theoretical and experimental values of γ. As expected, the γ value is proportional to the extinction ratio when extinction $>$ 10 dB. The agreement between theoretical and experimental γ is good.

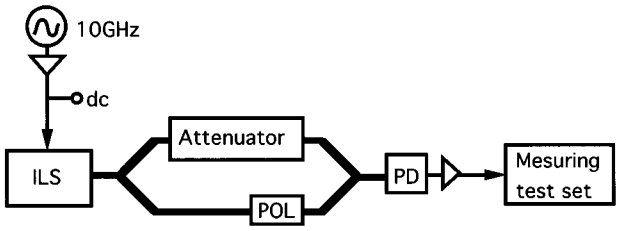

Fig. 7. The experimental setup for measuring the variation γ.

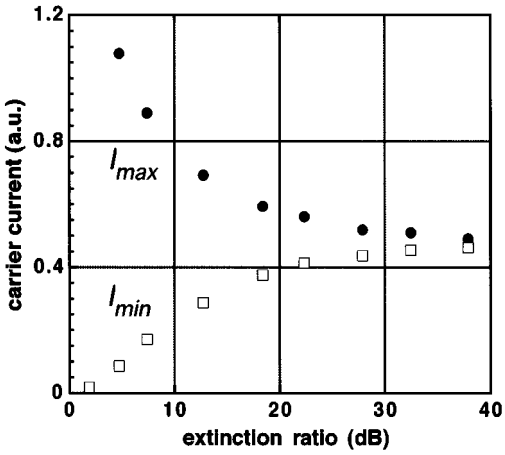

Fig. 8. Carrier current of the detected signal, $I_{\max}$ and $I_{\min}$.

Furthermore, we used the POL to make the polarizations of the two lights orthogonal to get a higher γ value. The variation γ becomes larger when the polarizations of the two lights are parallel, and becomes smaller when they are crossed. When the polarizations were orthogonal, the γ value increased by 20 dB. In our PSK experiment, β corresponds to the extinction ratio of each MZM if the two MZM's are regarded to have the same ratio. A MZM with a 30-dB extinction ratio may produce γ of 44 dB, which is suitable for practical radio communications. The phase difference, $\phi_1 - \phi_2$, depends on the temperature difference of the two paths and on their lengths. We therefore expect to reduce the variation by monolithic integration and temperature control.

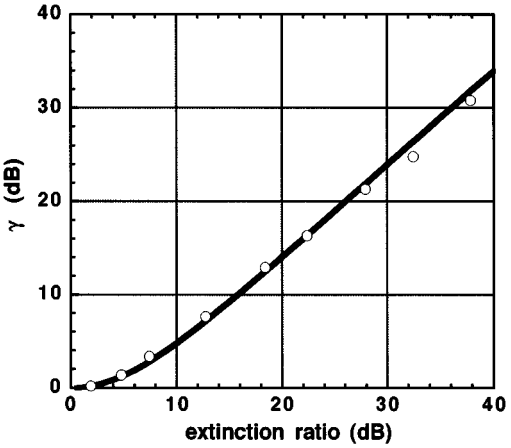

Fig. 9. Comparison of the theoretical (line) and experimental (squares) value of γ.

V. MPSK Modulation

MSPK modulation has already been used in radio systems. It can transmit $n = \log_2 M$ bits in a symbol time. Our modulation technique can be extended for MPSK modulation. Two configurations of 4PSK modulators are shown in Fig. 10: (a) is a cascade type and (b) a parallel type. Both types have ON-OFF switches (SW's) like MZM's.

The cascade type consists of a front block, which has SW-1 without a delay and SW-2 with delay of π, and a back block, which has SW-3 without a delay and SW-4 with delay of $\pi/2$. Sequential 2-bit data are input to each SW after encoding. An encoder converts the input signal into parallel data and adjusts the voltage for switching. Table II(a) lists the transmittance status and the assignment of phase delay $\phi$for a 2-bit signal. In both blocks, each SW pair is operated complementarily. For instance, when the output phase is assigned π for data of 10, the phase of the mm-wave SCM light is delayed in the front block, but it is no longer delayed in the back since only SW-2 and SW-3 are on. Furthermore, 8PSK and 16PSK are possible by adding another block.

The parallel type consists of four SW's and three delay lines. The SW's are connected in parallel. The delays on the SW-2, -3, and -4 paths are $\pi/2$, π, and $3\pi/2$, respectively. Table II(b) lists the transmittance status, combinations of data input, and phase delays. Only one SW of the four is on. For instance, when output phase is assigned π for data of 10, only SW-3 is on. Extensions to arbitrary multi-phase shift keying modulation are possible by connecting more SW's in parallel.

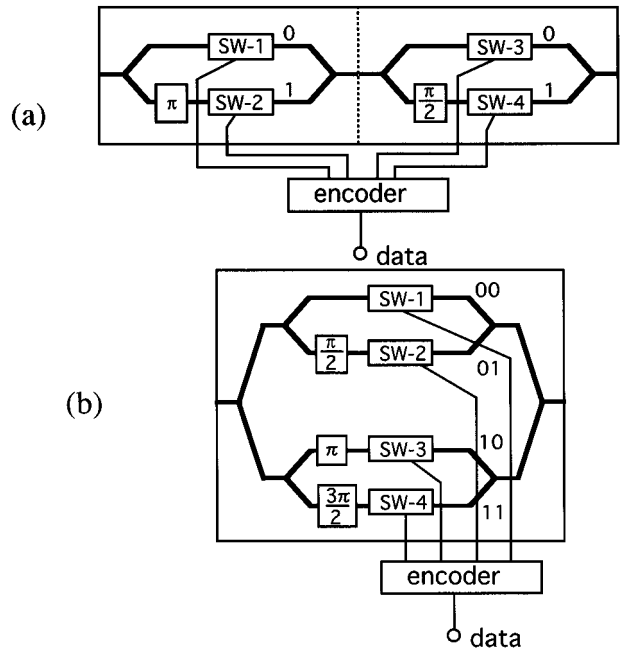

Fig. 10. Configurations of a 4PSK modulator. (a) Cacasde type and (b) parallel type.

VI. Summary

The novel PSK configuration for use at a central station in a fiber-optic radio links modulates mm-wave SCM light optically. It modulated a mm-wave carrier of 40-GHz frequency at bit rates of 2 Gbit/s without the need for high-speed electronic and optical devices. The error-free transmission of light was achieved over a 5-km optical fiber. Input light power over a 5-km DSF was −13.9 dBm and that over a back-to-back fiber was −13.7 dBm at the error rate of 1×10^{-9}. A 5-km transmission is sufficient for certain applications such as a wireless local area network. Furthermore, some of the solutions to overcome chromatic dispersion in an SMF are applicable to the SCM light source in our PSK modulator. These solutions will be a powerful system for implementing fiber-optic radio links.

We determined the relationship between the extinction ratio of the 2×1 switch and the variation of detected carrier power. It was confirmed that variation γ is proportional to extinction ratio β. And γ of over 40 dB was obtained for $\beta > 35$ dB when the polarizations of two paths were orthogonal. A combination of a commercial device, such as a MZM, and a polarization controller provides sufficient γ or carrier-to-noise ratio for practical radio communications. Extensions to a MPSK apparatus were also proposed.

Monolithic integration of this modulator and implementation by multiple access is under investigation.

TABLE II
THE TRANSMITTANCE STATUS OF EACH SW AND THE ASSIGNMENT OF PHASE DELAY FOR 2-BIT SIGNAL. (a) CASCADE TYPE, (b) PARALLEL TYPE. T_{SW1}: THE TRANSMITTANCE STATUS OF SW-1, T_{SW2}: THE TRANSMITTANCE STATUS OF SW-2, T_{SW3}: THE TRANSMITTANCE STATUS OF SW-3, T_{SW4}: THE TRANSMITTANCE STATUS OF SW-4

(a)

Data	T_{SW1}	T_{SW2}	T_{SW3}	T_{SW4}	ϕ
00	on	off	on	off	0
01	on	off	off	on	$\pi/2$
10	off	on	on	off	π
11	off	on	off	on	$3\pi/2$

(b)

Data	T_{SW1}	T_{SW2}	T_{SW3}	T_{SW4}	ϕ
00	on	off	off	off	0
01	off	on	off	off	$\pi/2$
10	off	off	on	off	π
11	off	off	off	on	$3\pi/2$

ACKNOWLEDGMENT

The authors would like to thank H. Iwamura and S. Mitachi for their encouragement.

REFERENCES

[1] W. E. Stephens and T. R. Joseph, "System characteristics of direct modulated and externally modulated RF fiber-optic links," *J. Lightwave Technol.*, vol. 5, pp. 380–387, 1987.
[2] H. Ogawa, "Microwave and millimeter-wave fiber optic technologies for subcarrier transmission systems," *IEICE Trans. Commun.*, vol. E-76-B, pp. 1078–1090, 1993.
[3] G. H. Smith, D. Novak, and Z. Ahmed, "Overcoming chromatic-dispersion effects in fiber-wireless systems incorporating external modulators," *IEEE Trans. Microwave Theory Tech.*, vol. 45, pp. 1401–1415, 1997.
[4] L. Noel, D. Wake, D. G. Moodie, D. D. Marcenac, L. D. Westbrook, and D. Nesset, "Novel techniques for high-capacity 60-GHz fiber-radio transmission systems," *IEEE Trans. Microwave Theory Tech.*, vol. 45, pp. 1416–1423, 1997.
[5] S. Fukushima, T. Ohno, Y. Doi, Y. Matsuoka, and H. Takeuchi, "New phase shift keying technique based on optical delay switching for microwave optical link," *IEEE Photon. Technol. Lett.*, vol. 8, 1999.
[6] K. Sato, K. Wakita, I. Kotaka, Y. Kondo, M. Yamamoto, and A. Takada, "Monolithic strained-InGaAsP multiple-quantum-well lasers with integrated electroabsorption modulators for active mode locking," *Appl. Phys. Lett.*, vol. 65, pp. 1–3, 1994.
[7] S. Arahira, Y. Matsui, and Y. Ogawa, "Mode-locking at very high repetition rates more than terahertz in passively mode-locked distributed-Bragg-reflector laser diodes," *IEEE J. Quantum Electron.*, vol. 32, pp. 1211–1224, 1996.
[8] K. Wakita, K. Yoshino, I. Kotaka, S. Kondo, and Y. Noguchi, "High speed, high efficiency modultor wity polarization insensitive and very low chirp," *Electron. Lett.*, vol. 31, pp. 2041–2042, 1995.
[9] K. Noguchi, H. Miyazawa, and O. Mitomi, "75 GHz broadband Ti:LiNbo3 optical modulator with ridge structure," *Electron. Lett.*, vol. 30, pp. 949–951, 1994.
[10] K. Kawano, M. Kohtoku, M. Ueki, T. Ito, S. Kondoh, Y. Noguchi, and Y. Hasumi, "Polarization-insensitive travelling-wave electrode electroabsorption (TW-EA) modulator with bandwidth over 50 GHz and driving voltage less than 2V," *Electron. Lett.*, vol. 33, pp. 1580–1581, 1998.
[11] G. H. Smith, D. Novak, and Z. Ahmed, "Technique for optical SSB generation to overcome dispersion penalties," *Electron. Lett.*, vol. 33, pp. 74–75, 1997.
[12] E. Vergnol, F. Devaux, D. Jahan, and D. Acarenco, "Fully integrated millimetric single-sideband lightwave source," *Electron. Lett.*, vol. 33, pp. 1961–1963, 1997.
[13] K. Sato, A. Hirano, M. Asobe, and H. Ishii, "Chirp-compensated 40 GHz semiconductor modelocked lasers integrated with chirped gratings," *Electron. Lett.*, vol. 34, pp. 1944–1946, 1998.
[14] D. Wake, C. R. Lima, and P. A. Davis, "Transmission of 60-GHz signals over 100 km of optical fiber using a dual mode semiconductor laser source," *IEEE Photon. Technol. Lett.*, vol. 8, pp. 578–580, 1996.
[15] H. Takeuchi, K. Tsuzuki, K. Sato, M. Yamamoto, Y. Itaya, and A. Sano, "NRZ operation at 40 Gbit/s of a compact module containing an MQW electroabsorption modulator integrated with a DFB laser," *IEEE Photon. Technol. Lett.*, vol. 9, pp. 572–574, 1997.
[16] A. F. Elrefaie, R. E. Wagner, D. A. Atlas, and D. G. Daut, "Chromatic dispersion limitations in coherent lightwave transmission systems," *J. Lightwave Technol.*, vol. 6, pp. 704–709, 1988.
[17] F. Koyama and K. Iga, "Frequency chirping in external modulators," *J. Lightwave Technol.*, vol. 6, pp. 87–92, 1988.
[18] F. Devaux, Y. Sorel, and J. F. Kerdiles, "Simple measurement of fiber dispersion and of chirp parameter of intensity modulated light emitter," *J. Lightwave Technol.*, vol. 11, pp. 1937–1940, 1993.

Yoshiyuki Doi was born in Hyogo, Japan, in 1973. He received the B.S. and M.S. degrees in physics from Shinshu University, Nagano, Japan, in 1995 and 1997, respectively.

In 1997, he joined NTT Opto-electronics Laboratories, Japan, and has been engaged in high-speed opto-electronics devices. He is currently with NTT Photonics Laboratories, where his research interests are optical devices used in fiber radio systems.

Mr. Doi is a member of the Institute of Electronics, Information and Communication Engineers (IEICE) of Japan.

Seiji Fukushima received the B.S., M.S., and Ph.D. degrees in electric engineering from Kyushu University, Fukuoka, Japan, in 1984, 1986, and 1993, respectively.

In 1986, he joined NTT Opto-electronics Laboratories, Japan, and became engaged in research of spatial light modulators and optical computing systems. From 1995 to 1997, he was engaged in research of high-speed optical interconnection for the integrated circuits in NTT System Electronics Laboratories. In 1997, he began studying devices for fiber radio systems in NTT Photonics Laboratories.

Dr. Fukushima is a member of the Optical Society of America (OSA), the Institute of Electronics, Information and Communication Engineers (IEICE) of Japan, and the Japan Society of Applied Physics.

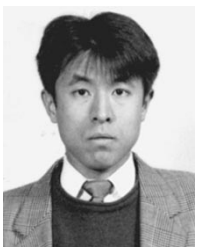

Tetsuichiro Ohno (M'98) received the B.E. and M.E. degrees from Osaka University, Japan, in 1989 and 1991, respectively, and the Ph.D. degree from Shizuoka University, Japan, in 1999.

In 1991, he joined NTT Opto-electronics Laboratories, Japan, and has been engaged in optical devices. He is currently with NTT Photonics Laboratories, Japan, where his current interests are in the area of optical devices used in fiber radio systems.

Dr. Ohno is a member of IEEE/LEOS.

Yutaka Matsuoka (M'92) received B.S. and M.S. degrees in physics from Tokyo Institute of Technology, Tokyo, Japan, in 1974 and 1976, respectively.

In 1976, he joined Musashino Electrical Communication Laboratory, Nippon Telegraph and Telephone Public Corporation, Japan, where he worked on electrical characterization of Si and GaAs substrates. From 1982 to 1986, his research focused on high-speed GaAs MESFET's and IC's. He is currently with NTT Photonics Laboratories, where his research interests include high-performance photodiodes, InP-based heterostructure bipolar transistors, OEIC's, and micro/millimeter-wave photonics.

Hiroaki Takeuchi received the B.S., M.S., and Ph.D. degrees in applied physics from Waseda University, Tokyo, Japan, in 1981, 1983, and 1991 respectively.

In 1983, he joined Atsugi Electrical Communication Laboratory, Nippon Telegraph and Telephone Public Corporation, Japan, where he had been working on MBE growth of III–V materials and many variety of semiconductor integrated optical devices. He is currently with NTT Photonics Laboratories, Japan, where his research interests mainly include electroabsorption modulators and its integrated devices.